AIP Journal of Applied Physics

Effect of antimony incorporation on the density, shape, and luminescence of InAs quantum dots

J. F. Chen, C. H. Chiang, Y. H. Wu, L. Chang, and J. Y. Chi

Citation: Journal of Applied Physics **104**, 023509 (2008); doi: 10.1063/1.2959598
View online: http://dx.doi.org/10.1063/1.2959598
View Table of Contents: http://scitation.aip.org/content/aip/journal/jap/104/2?ver=pdfcov
Published by the AIP Publishing

Articles you may be interested in

Interface properties of InAs quantum dots produced by antimony surfactant-mediated growth: Etching of segregated antimony and its impact on the photoluminescence and lasing characteristics
Appl. Phys. Lett. **94**, 103116 (2009); 10.1063/1.3099902

Structural and optical properties of InP quantum dots grown on GaAs(001)
J. Appl. Phys. **101**, 073508 (2007); 10.1063/1.2718869

High density In As Ga As quantum dots with enhanced photoluminescence intensity using antimony surfactant-mediated metal organic chemical vapor deposition
Appl. Phys. Lett. **89**, 183124 (2006); 10.1063/1.2385209

Topological characteristics of InAs quantum dot with GaInAs cover using Sb surfactant
Appl. Phys. Lett. **88**, 183109 (2006); 10.1063/1.2200395

Sb surfactant effect on GaInAs/GaAs highly strained quantum well lasers emitting at 1200 nm range grown by molecular beam epitaxy
J. Appl. Phys. **96**, 44 (2004); 10.1063/1.1760841

Re-register for Table of Content Alerts

Create a profile.

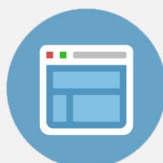

Sign up today!

[This article is copyrighted as indicated in the article. Reuse of AIP content is subject to the terms at: http://scitation.aip.org/termsconditions. Downloaded to] IP: 140.113.38.11 On: Wed, 30 Apr 2014 23:00:17

JOURNAL OF APPLIED PHYSICS **104**, 023509 (2008)

Effect of antimony incorporation on the density, shape, and luminescence of InAs quantum dots

J. F. Chen,[1,a)] C. H. Chiang,[1] Y. H. Wu,[2] L. Chang,[2] and J. Y. Chi[3]
[1]*Department of Electrophysics, National Chiao Tung University, 30050 Hsinchu, Taiwan, Republic of China*
[2]*Department of Materials Science and Engineering, National Chiao Tung University, Hsinchu 30050, Taiwan*
[3]*Industrial Technology Research Institute (OES/ITRI), Hsinchu 31015, Taiwan*

(Received 14 December 2007; accepted 27 May 2008; published online 18 July 2008)

This work investigates the surfactant effect on exposed and buried InAs quantum dots (QDs) by incorporating Sb into the QD layers with various Sb beam equivalent pressures (BEPs). Secondary ion mass spectroscopy shows the presence of Sb in the exposed and buried QD layers with the Sb intensity in the exposed layer substantially exceeding that in the buried layer. Incorporating Sb can reduce the density of the exposed QDs by more than two orders of magnitude. However, a high Sb BEP yields a surface morphology with a regular periodic structure of ellipsoid terraces. A good room-temperature photoluminescence (PL) at ~1600 nm from the exposed QDs is observed, suggesting that the Sb incorporation probably improves the emission efficiency by reducing the surface recombination velocity at the surface of the exposed QDs. Increasing Sb BEP causes a blueshift of the emission from the exposed QDs due to a reduction in the dot height as suggested by atomic force microscopy. Increasing Sb BEP can also blueshift the ~1300 nm emission from the buried QDs by decreasing the dot height. However, a high Sb BEP yields a quantum well-like PL feature formed by the clustering of the buried QDs into an undulated planar layer. These results indicate a marked Sb surfactant effect that can be used to control the density, shape, and luminescence of the exposed and buried QDs. © *2008 American Institute of Physics*.
[DOI: 10.1063/1.2959598]

I. INTRODUCTION

Self-assembled InAs quantum dots (QDs)[1–14] are of great interest for scientific studies and practical applications. One of the important issues for device applications is the ability to modify the size, shape, and density of the dots. However, the self-assembled Stranski–Krastanov method of growth offers very limited modification. Motivated by the beneficial results of the incorporation of antimony (Sb) as a surfactant[15–18] into a strained InGaAs quantum well (QW) to extend the range of emission wavelengths, the incorporation of Sb (Refs. 19–23) or bismuth[24] in InAs or in InGaAs QDs has been recently investigated. Matsuura *et al.*[21] observed a decrease in the dot density upon the incorporation of Sb in InGaAs QDs and attributed this decrease to an Sb surfactant effect that can extend planar growth and suppress dot formation. A predeposition of dilute Sb before the growth of InAs QDs by metalorganic vapor-phase epitaxy was found to increase the dot size.[23] Very recently, a long emission wavelength of ~1.6 μm at room temperature has been achieved by capping InAs QDs with (In)GaAsSb layer.[12–14] This wavelength extension is explained by a development of type-II energy alignment. These experimental results seem to indicate that an incorporation of Sb directly into the QDs can lead to an Sb surfactant effect while an incorporation of Sb into the capping layer of the QDs can extend the emission wavelength. To understand the details of the surfactant effect, we have directly incorporated various amounts of Sb into buried and exposed InAs QDs and characterized their optical and structural properties using photoluminescence (PL), atomic force microscopy (AFM), and transmission electron microscopy (TEM). Secondary ion mass spectroscopic (SIMS) depth profiling is also used to analyze the Sb distribution.

II. EXPERIMENTS

InAs(Sb) QDs were grown on n^+-GaAs(100) substrates by molecular beam epitaxy using a Riber Epineat machine. The QDs were formed by depositing a 2.72 ML-thick InAs(Sb) layer at 485 °C at a growth rate of 0.256 Å/s. Three Sb contents with beam equivalent pressures (BEPs) of 1.4×10^{-8}, 1.8×10^{-8}, and 6×10^{-8} torr, supplied from an Sb cracker, were incorporated into the InAs QD growth. Then, the QDs were capped with a 50 Å $In_{0.15}Ga_{0.85}As$ layer grown at 485 °C at a growth rate of 1.88 Å/s. These buried QDs are sandwiched between two 0.3-μm-thick Si-doped GaAs (6×10^{16} cm^{-3}) layers. For AFM characterizations, similar QDs capped with a 50 Å $In_{0.15}Ga_{0.85}As$ layer were also grown on sample surface. Details of the growth of the QDs can be found elsewhere.[22] PL measurements were made using a double frequency yttrium aluminum garnet: Nd laser at 532 nm.

III. MEASUREMENT AND RESULTS

Figure 1 shows the SIMS depth profiles for Sb BEP of 6×10^{-8} torr. The profiles show the presence of Sb near the sample surface and at a depth of 0.3 μm, suggesting a suc-

a)Electronic mail: jfchen@cc.nctu.edu.tw.

 © 2008 American Institute of Physics

[This article is copyrighted as indicated in the article. Reuse of AIP content is subject to the terms at: http://scitation.aip.org/termsconditions. Downloaded to] IP: 140.113.38.11 On: Wed, 30 Apr 2014 23:00:17

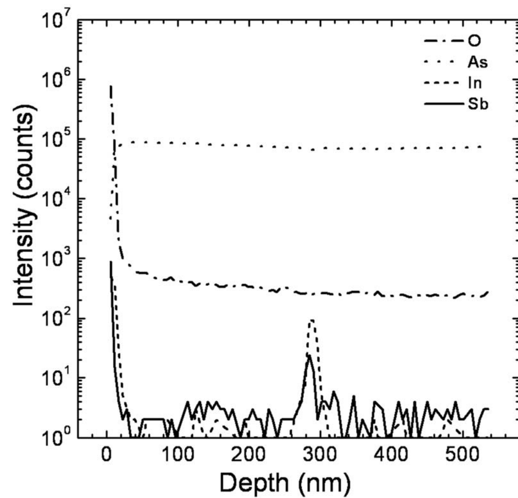

FIG. 1. SIMS depth profiles of ion intensities for InAs(Sb) QDs with Sb BEP of 6×10^{-8} torr. The profiles reveal the presence of Sb in the exposed and buried QD layers. The intensity in the exposed layer substantially exceeds that in the buried layer, suggesting Sb segregation at growth front.

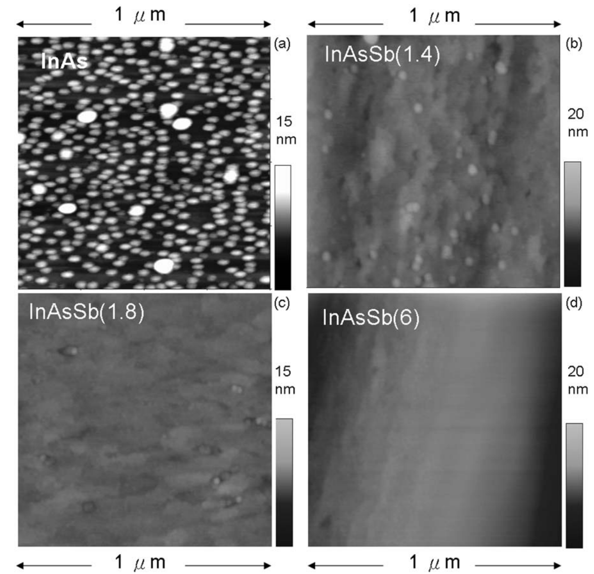

FIG. 2. (a)–(d) Representative 1×1 μm^2 AFM images of the exposed QDs with Sb BEPs of 0, 1.4×10^{-8}, 1.8×10^{-8}, and 6×10^{-8} torr, respectively. Sb incorporation can reduce the dot density by more than two orders of magnitude.

cessful incorporation of Sb in the exposed and buried layers. However, the three dimensional nature of the QDs is such that the detected Sb may not be completely inside the QDs. A significant amount of Sb may be present in the intervening GaAs. Although the exposed and buried layers were grown similarly, the Sb intensity in the exposed layer substantially exceeds that in the buried layer. Similar profile is observed for In intensity. The observed Sb intensity in the exposed layer depends linearly on the Sb BEP, suggesting that Sb can be incorporated into the exposed layer without saturation effect. However, the Sb intensity in the buried layer only slightly exceeds the background Sb noise. Decreasing the Sb BEP further weakens the Sb intensity in the buried layer. For a low Sb BEP of 1.4×10^{-8} torr, the Sb intensity in the buried layer is close to a background level. Because of the very low intensity, no reliable relationship between the BEP and the Sb intensity can be obtained in the buried layer. The low Sb intensity in the buried layer suggests a weak Sb incorporation. Because Sb concentration is dilute in the buried QDs, the resulting increase in the QD/GaAs lattice mismatch and the decrease in the band gap in the buried QDs due to Sb occupation of As sublattice are considered insignificant.

Figures 2(a)–2(d) show the representative 1×1 μm^2 AFM images of the exposed QDs with Sb BEPs of 0, 1.4×10^{-8}, 1.8×10^{-8}, and 6×10^{-8} torr, respectively [denoted as InAs, InAsSb(1.4), InAsSb(1.8), and InAsSb(6), respectively]. Without Sb, random QDs with a density of 3×10^{10} cm^{-2} can be seen along with a few large clusters. An Sb BEP of 1.4×10^{-8} torr can reduce the dot density to 3.5×10^{9} cm^{-2}; an Sb BEP of 1.8×10^{-8} torr further reduces it to 6×10^{8} cm^{-2}. The reflection high-energy electron diffraction patterns show delayed QD formation upon Sb incorporation.[22] Therefore, the decrease in dot density is explained by an Sb surfactant effect that can extend two dimensional (2D) growth and suppress dot formation. Further increasing Sb BEP to 6×10^{-8} torr changes the surface morphology to ellipsoid terraces of height ~9 nm, length ~4.5 μm, and width ~1.3 μm, as shown in Fig. 3. Thus, a large Sb BEP worsens the surface morphology and a significant amount of the deposited material tends to form these thick terraces, rather than a thin wetting layer. A few QDs are observed on top of these terraces. The dot density is too low to be determined accurately by AFM. However, since the AFM picture shows less than one dot in an area of 1×1 μm^2, the estimated density is less than 1×10^{8} cm^{-2}. This density is more than two orders of magnitude lower than that of the Sb-free QDs. Cross-sectional TEM reveals a typical dot with a height of about 3 nm and a diameter of 20 nm. This AFM result shows that Sb incorporation can effectively reduce the density of the exposed QDs, as previously observed.[21] However, increasing the Sb BEP to 6×10^{-8} torr yields a surface morphology with a regular periodic structure of ellipsoid terraces.

The density reduction is accompanied by concomitant size and shape modifications. The Sb-free QDs have an average lateral diameter of 50 nm and a height of 10 nm. An Sb BEP of 1.4×10^{-8} torr reduces the height to ~5 nm without significantly affecting the lateral diameter. Increasing the Sb BEP to 1.8×10^{-8} torr reduces the lateral diameter and height to 35 and 3 nm, respectively. Further increasing the Sb

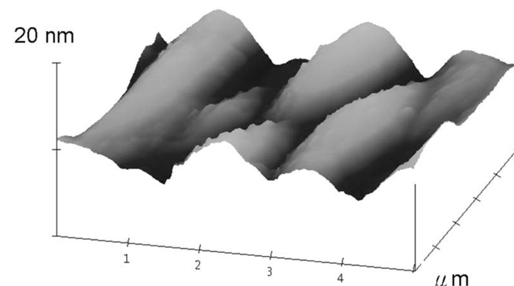

FIG. 3. For a high Sb BEP of 6×10^{-8} torr, the surface morphology comprises ellipsoid terraces of height ~9 nm, length ~4.5 μm, and width ~1.3 μm.

[This article is copyrighted as indicated in the article. Reuse of AIP content is subject to the terms at: http://scitation.aip.org/termsconditions. Downloaded to] IP: 140.113.38.11 On: Wed, 30 Apr 2014 23:00:17

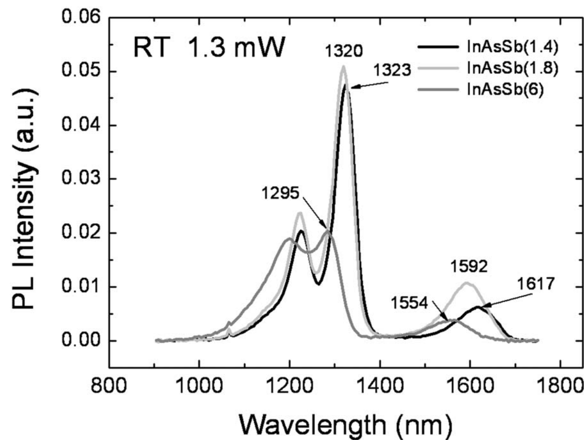

FIG. 4. Room-temperature PL spectra for Sb BEPs of 1.4×10^{-8}, 1.8×10^{-8}, and 6×10^{-8} torr at an excitation power of 1.3 mW. Each spectrum displays two groups of peaks: the peaks at $\sim$1300 nm are from the buried QDs and the peaks at $\sim$1600 nm are from the exposed QDs. Both groups exhibit a blueshift as the Sb BEP increases because the dot height decreases.

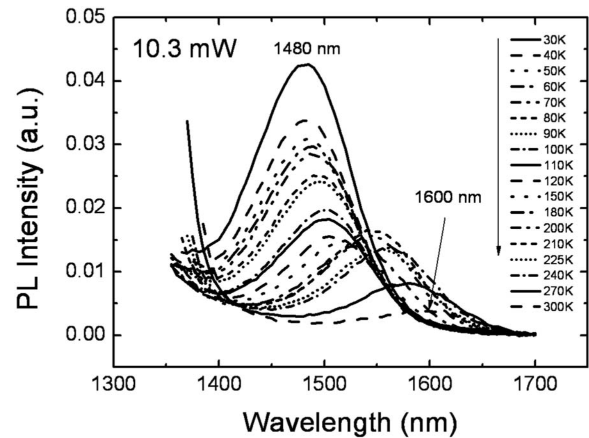

FIG. 5. Temperature-dependent PL spectra of the exposed QDs with Sb BEP of 1.4×10^{-8} torr. The emission improves as temperature decreases, which improvement is accompanied by a blueshift of 62 meV (from 300 to 30 K), consistent with the Varshini rule.

BEP to 6×10^{-8} torr reduces the lateral diameter to $\sim$20 nm without significantly affecting the height. This dot size reduction is consistent with the surfactant's suppression of the growth of the QD and thus the Sb surfactant effect markedly affects the growth of the exposed QDs. Although the lateral dimension is reduced as the Sb BEP increases, the ratio of the lateral diameter to the height exceeds significantly that of the Sb-free QDs and the ratio increases with Sb BEP, and so Sb incorporation can elongate the shape of the QD. These results show a significant Sb surfactant effect affecting the growth of the exposed QDs. The SIMS profile shows a high Sb intensity in the exposed layer and the intensity can be linearly varied by changing the Sb BEP. Thus, this surfactant effect can be utilized for the effective modification of the density and shape of the QDs.

Figure 4 shows the 300 K PL spectra for Sb BEPs of 1.4×10^{-8}, 1.8×10^{-8}, and 6×10^{-8} torr, respectively. Each spectrum displays two groups of peaks. The peaks at $\sim$1300 nm are from the buried QDs and the peaks at $\sim$1600 nm are from the exposed QDs since they disappear after slight chemical etching on the sample surface. The PL spectra of Sb-free QDs exhibit a similar 1300 nm emission without the 1600 nm emission. There are two possible contributions for the long wavelength in the exposed QDs: strain relaxation and Sb incorporation. Considering a significant compressive strain in the buried QDs, strain relaxation in the exposed QDs[11] can lead to a wavelength extension. Previous studies have shown that uncapped InGaAs QDs on a GaAs surface could emit a long wavelength near 1500 nm.[11] Another contribution is due to Sb incorporation since the SIMS profile shows a high Sb incorporation in the exposed QD layer than in the buried layer. A high Sb concentration can substantially decrease the band gap of the InAs QDs and result in a wavelength extension. Another possibility is that the incorporated Sb may segregate to the InGaAs capping layer, forming an InGaAsSb capping layer on the QDs. A long wavelength of 1600 nm was previously observed in InAs QDs capping with an (In)GaAsSb layer due to the formation of type-II energy alignment.[12–14] Further investigation is needed to clarify the detailed origin for the wavelength extension. The emission from the exposed QDs is blueshifted from 1617 to 1554 nm as Sb BEP increases. This blueshift is attributed to a reduction in the dot height, as suggested by the AFM observation. Thus, the shift in the PL emission for the exposed QDs as Sb BEP is varied is mainly governed by the surfactant effect. Figure 5 plots the temperature dependence of $\sim$1600 nm emission with Sb BEP of 1.4×10^{-8} torr. As temperature is lowered, the emission intensity increases and a blueshift of 63 meV (Varshini rule)[25] is observed, reflecting good emission efficiency for such a long wavelength. Due to strong surface recombination velocity, it is difficult for the exposed QDs to exhibit good emission efficiency. Saito *et al.*[11] reported that In segregation on the surface InGaAs QDs could improve PL intensity by reducing surface recombination velocity and suppressing carrier loss at the surface of QDs. However, in our case, the improvement in the emission efficiency shall be related to Sb since no 1600 nm emission was observed in Sb-free QDs. Thus, the improvement in the 1600 nm emission efficiency is tentatively explained by a high Sb concentration on the surface of the QDs. These results show that, with Sb incorporation, the exposed QDs can achieve a long emission of $\sim$1600 nm with good emission efficiency.

Unlike the exposed QDs, the buried QDs emit a wavelength of $\sim$1300 nm. Similar emission wavelength is observed in buried Sb-free QDs. Thus, the Sb incorporation does not affect the emission wavelength much, probably due to a weak Sb incorporation as shown by the SIMS profile. Increasing Sb BEP in the buried QDs leads to a blueshift of the emission, as shown in Fig. 4. The near 1300 nm spectra show a doublet feature similar to the ground and first-excited transitions of the QDs. Increasing Sb BEP blueshifts the ground transition from 1323 to 1295 nm. Hence, the change in the wavelength is not due to the band gap reduction or type-II transition of Sb incorporation. This blueshift is explained by the reduction in the height of the buried QDs (to be shown by TEM picture), suggesting an Sb surfactant effect. The similar peak intensities of the ground transitions for BEPs of 1.4×10^{-8} and 1.8×10^{-8} torr suggest comparable

[This article is copyrighted as indicated in the article. Reuse of AIP content is subject to the terms at: http://scitation.aip.org/termsconditions. Downloaded to] IP: 140.113.38.11 On: Wed, 30 Apr 2014 23:00:17

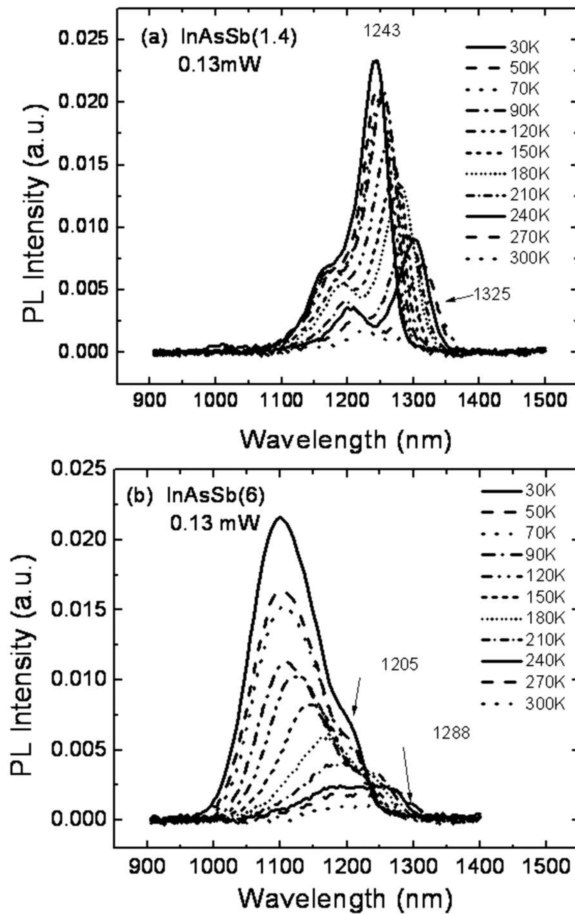

FIG. 6. Temperature-dependent PL spectra for Sb BEP of (a) 1.4×10^{-8} and (b) 6×10^{-8} torr. While typical ground-transition dominated PL spectra are observed for BEP of 1.4×10^{-8} torr, the PL spectra for Sb BEP of 6×10^{-8} torr display an enormously broad high-energy transition at low temperature, which is attributed to an emission from a QW-like layer due to clustering of the QDs.

dot densities. The much lower intensity of the ground transition for an Sb BEP of 6×10^{-8} torr reflects a lower dot density. This trend is similar to that observed in the exposed QDs although the reduction is not that strong. Thus, the buried layer has a weaker Sb surfactant effect than the exposed layer, consistent with a weaker Sb incorporation, as shown by the SIMS profile. For low Sb (BEP=1.4×10^{-8} and 1.8×10^{-8} torr), as the excitation power increases, the first-excited transition gains increasing relevance and eventually dominates the ground transition; this change is accompanied by the emergence of the second-excited transition. These features are typically observed in one predominant QD family. Thus, the QDs for low Sb BEP are rather homogeneous. However, for a high Sb BEP of 6×10^{-8} torr, although a typical QD doublet feature is observed at high temperature, the spectra at low temperature differ markedly.

Figures 6(a) and 6(b) compare the temperature-dependent PL spectra of Sb BEPs of 1.4×10^{-8} and 6×10^{-8} torr. As temperature is lowered, the PL spectra for a high Sb BEP of 6×10^{-8} torr show anomalous temperature dependence. The first-excited transition exhibits an abnormally large blueshift of 94 meV (from 300 to 30 K) versus a blueshift of ~40 meV for a low Sb BEP of 1.4×10^{-8} torr.

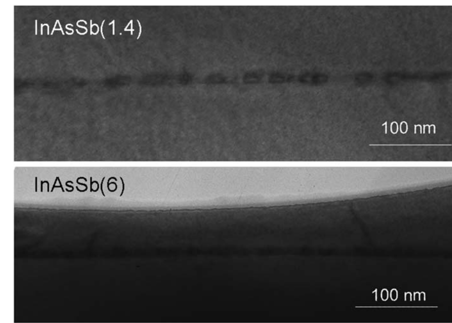

FIG. 7. Cross-sectional TEM image of the QDs for Sb BEPs of 1.4×10^{-8} and 6×10^{-8} torr. Separated QDs with mean height of 25 nm are formed for an Sb BEP of 1.4×10^{-8} torr, while the QDs for Sb BEP of 6×10^{-8} torr cluster into an undulated QW-like layer with a thickness of 12–15 nm.

This abnormally large blueshift is accompanied by an enormous intensity enhancement and linewidth broadening, causing the PL spectra to be dominated by the enormous peak centered at 1100 nm. The integrated intensity of this peak is more than three times higher than that of the ground transition for Sb BEP of 1.4×10^{-8} torr. This anomalous feature cannot be explained simply by the very wide size dispersion of the QDs. A high-lying energy level with a considerable density must be present to explain the enormously broad 1100 nm peak. This energy level is attributed to a QW-like level, as suggested by the cross-sectional TEM picture in Fig. 7. For a low Sb of 1.4×10^{-8} torr, separated QDs with a mean height of 25 nm can be clearly seen. Increasing the Sb BEP to 6×10^{-8} torr substantially reduces the height of the QDs and increases their lateral dimension, causing clustering of the QDs into an undulated QW-like layer with a thickness of 12–15 nm. The reduction in the height of the QDs explains the observed blueshift of the ~1300 nm emission as Sb BEP is increased. Notably, the TEM picture shows that the bottom interface of the QW-like layer is relatively flat in comparison with the undulated upper interface. Hence, the clustering mainly occurs in the base of the QDs and the top of the QDs has not yet emerged together. The structure is similar to QDs on a wetting layer with an effective thickness being much thicker than a typical wetting layer for Sb-free QDs but thinner than the height of the QDs. Hence, the emission wavelength from the QW-like layer is expected to be longer than that ~900 nm from a typical wetting layer for Sb-free QDs but shorter than the ground transition (~1300 nm) of the QDs. This is more or less consistent with the observed anomalous peak centered at 1100 nm. The large broadness of this peak is indicative of the undulated interface of the QW-like layer. At high temperatures, most of the carriers are confined in the QDs and the PL spectra are dominated by their emissions. As temperature is lowered, carriers begin to fill in the QW-like level, and thus the related emission gains increasing relevance, leading to the QW-like PL spectra at low temperature. The formation of this QW-like layer further confirms an Sb surfactant effect that governs the growth of the buried QDs. Both the exposed and buried layers exhibit Sb surfactant effect: A reduction in dot density and a blueshift of PL emission with increasing Sb BEP, and for a high Sb concentration, the exposed layer yields surface

[This article is copyrighted as indicated in the article. Reuse of AIP content is subject to the terms at: http://scitation.aip.org/termsconditions. Downloaded to] IP: 140.113.38.11 On: Wed, 30 Apr 2014 23:00:17

morphology of ellipsoid terraces and the buried QDs are clustered into a QW-like layer. In view of the strong reduction in the dot density and the significant morphology change, the exposed layer shows a stronger surfactant effect than the buried layer, consistent with the relative Sb intensities observed by the SIMS profile. The weak Sb intensity observed in the buried QDs by the SIMS profile strongly suggests that it is not necessary to incorporate Sb into the QD layer in order to have surfactant effect.

IV. CONCLUSIONS

In summary, Sb incorporation into the InAs QDs is shown to modify the density, shape, and PL spectra of the QDs by the Sb surfactant effect. The density of the exposed QDs can be reduced by more than two orders of magnitude by Sb incorporation. This decrease in density is accompanied by a reduction in the height of the QDs and a related PL blueshift. The exposed QDs exhibit a long emission wavelength of ~1600 nm with good emission efficiency at 300 K, suggesting that the Sb concentration at the surface can probably reduce the surface recombination velocity of the QDs. However, as the Sb BEP is further increased, the surface morphology yields a regular periodic structure of ellipsoid terraces and the buried QDs are simultaneously clustered into an undulated 2D layer, giving rise to anomalous QW-like emission at low temperature. These results indicate a marked Sb surfactant effect to suppress the growth of the QDs.

ACKNOWLEDGMENTS

The authors would like to thank the National Science Council of Taiwan (Contract No. NSC-94-2112-M-009-029) and the Ministry of Education under the ATU program for financially supporting this research. Dr. R. S. Hsiao is appreciated for sample fabrication.

[1] F. Heinrichsdorff, M.-H. Mao, N. Kirstaedter, A. Krost, and D. Bimberg, Appl. Phys. Lett. **71**, 22 (1997).
[2] G. Yusa and H. Sakaki, Electron. Lett. **32**, 491 (1996).
[3] D. J. Eaglesham and M. Cerullo, Phys. Rev. Lett. **64**, 1943 (1990).
[4] D. Leonard, K. Pond, and P. M. Petroff, Phys. Rev. B **50**, 11687 (1994).
[5] S. Guha, A. Madhukar, and K. C. Rajkumar, Appl. Phys. Lett. **57**, 2110 (1990).
[6] J. M. Moison, F. Houzay, F. Barthe, and L. Leprince, Appl. Phys. Lett. **64**, 196 (1994).
[7] M. V. Maximov, A. F. Tsatsulnikov, B. V. Volovik, D. A. Bedarev, A. Yu. Egorov, A. E. Zhukov, A. R. Kovsh, N. A. Bert, V. M. Ustinov, P. S. KopeV, Zh. I. Alferov, N. N. Ledentsovb, D. Bimberg, I. P. Soshnikovc, and P. Werner, Appl. Phys. Lett. **75**, 2347 (1999).
[8] C. W. Snyder, J. F. Mansfield, and B. G. Orr, Phys. Rev. B **46**, 9551 (1992).
[9] D. Leonard, M. Krishnamurthy, C. M. Reaves, S. P. Denbaars, and P. M. Petroff, Appl. Phys. Lett. **63**, 3203 (1993).
[10] H. Shoji, K. Mukai, N. Ohtsuka, M. Sugawara, T. Uchida, and H. Ishikawa, IEEE Photon. Technol. Lett. **7**, 1385 (1995).
[11] H. Saito, K. Nishi, and S. Sugou, Appl. Phys. Lett. **73**, 2742 (1998).
[12] T. Matsuura, T. Miyamoto, T. Kageyama, M. Ohta, Y. Matsui, T. Furuhata, and F. Koyama, Jpn. J. Appl. Phys., Part 2 **43**, L82 (2003).
[13] J. M. Ripalda, D. Granados, Y. Gonzalez, A. M. Sanchez, S. I. Molina, and J. M. Garcia, Appl. Phys. Lett. **87**, 202108 (2005).
[14] H. Y. Liu, M. J. Steer, T. J. Badcock, D. J. Mowbray, M. S. Skolnick, F. Suarez, J. S. Ng, M. Hopkinson, and J. P. R. David, J. Appl. Phys. **99**, 046104 (2006).
[15] T. Kageyama, T. Miyamoto, M. Ohta, T. Matsuura, Y. Matsui, T. Furuhata, and F. Koyama, J. Appl. Phys. **96**, 44 (2004).
[16] J. C. Harmand, L. H. Li, G. Patriarche, and L. Travers, Appl. Phys. Lett. **84**, 3981 (2004).
[17] X. Yang, M. J. Jurlovic, J. B. Heroux, and W. I. Wang, Appl. Phys. Lett. **75**, 178 (1999).
[18] H. Shimizu, K. Kumada, S. Uchiyama, and A. Kasukawa, Electron. Lett. **36**, 1379 (2000).
[19] A. Krier, X. L. Huang, and A. Hammiche, Appl. Phys. Lett. **77**, 3791 (2000).
[20] K. Suzuki and Y. Arakwa, Phys. Status Solidi B **224**, 139 (2001).
[21] T. Matsuura, T. Miyamoto, T. Kageyama, M. Ohta, Y. Matsui, T. Furuhata, and F. Koyama, Jpn. J. Appl. Phys., Part 2 **43**, L605 (2004).
[22] J. F. Chen, R. S. Hsiao, W. D. Huang, Y. H. Wu, L. Chang, J. S. Wang, and J. Y. Chi, Appl. Phys. Lett. **88**, 233113 (2006).
[23] Y. Sun, S. F. Cheng, G. Chen, R. F. Hicks, J. G. Cederberg, and R. M. Biefeld, J. Appl. Phys. **97**, 053503 (2005).
[24] B. N. Zvonkov, I. A. Karpovich, N. V. Baidus, D. O. Filatov, S. V. Morozov, and Y. Y. Gushina, Nanotechnology **11**, 221 (2000).
[25] Y. P. Varshni, Physica (Amsterdam) **34**, 149 (1967).

[This article is copyrighted as indicated in the article. Reuse of AIP content is subject to the terms at: http://scitation.aip.org/termsconditions. Downloaded to] IP: 140.113.38.11 On: Wed, 30 Apr 2014 23:00:17